Article

Molecular dynamics simulations of zfP2X4 receptors

Kalyan Immadisetty[1] and Peter Huskey[1,*]

[1]Stritch School of Medicine, Maywood IL 60153

[*]Correspondence: pkekeneshuskey@luc.edu

ABSTRACT The ATP activated P2X4 receptor plays a prominent role in pain perception and modulation and thus may constitute an alternative therapeutic target for controlling pain. Given the biomedical relevance of P2X4 receptors, and poor understanding of molecular mechanisms that describe its gating by ATP, fundamental understanding of functional mechanism of these channels is warranted. Through classical all-atom molecular dynamics (MD) simulations we investigated the number of ATP molecules required to open (activate) the receptor for it to conduct ions. Since crystal structures of human P2X4 are not yet available, the crystal structures of highly-homologous zebrafish P2X4 (zfP2X4) structures were utilized for this study. It has been identified that at least two ATP molecules are required to prevent the open state receptor collapsing back to a closed state. Additionally, we have discovered two metal binding sites, one at the intersection of the three monomers in the ectodomain (MBS1) and the second one near the ATP binding site (MBS2), both of which are occupied by the potassium ions. This observation draws its comparison to the gulf coast P2X receptor that it possess the same two metal binding sites, however, MBS1 and MBS2 in this receptor are occupied by zinc and magnesium, respectively.

1 INTRODUCTION

Purinergic (P2X) receptors are ligand-gated cation channels that reside in the plasma membrane (1). P2X4 receptors are expressed in almost all mammalian tissues (2). P2X4 receptor is activated by adenosine triphosphate (ATP) (3–6), during which the channel opens and allows rapid flow of ions such as calcium (Ca^{2+}), magnesium (Mg^{2+}) and potassium (K^{+}) (6). P2X4 receptor exhibits high Ca^{2+} permeability and contributes to depolarization of the cell membrane, whereby various Ca^{2+} sensitive intracellular processes are triggered (6–8). P2X4 receptors are implicated in the regulation of cardiac function, ATP-mediated cell death, synaptic strengthening, activating of the inflammasome in response to injury and multiple sclerosis (5, 9–12). The P2X4 receptors are linked to neuropathic pain mediated by microglia (13, 14). Studies have found that P2X4 receptors are upregulated following injury (15). More importantly, P2X4 activation is both necessary and sufficient for neuropathic pain (16).

Despite their biomedical relevance, several structural (role of intracellular fragments and pore dilation) and functional aspects (activation mechanism, allosteric modulation by agonists such as ivermectin (IVM), the number of ATP needed to activate the channel, and desensitization) of P2X4 channels are still debated (17, 18). This makes it difficult to understand the extent to which P2X4 activation drives cellular responses and its potential druggability. A pressing limitation is the lack of human P2X4 crystal structures. However, zfP2X4 structures have been crystallized in multiple relevant conformations and in different functional states (19, 20). zfP2X4 shares ~59% sequence identity with human P2X4 (17) and has been shown to

form functional homomeric channels with properties comparable to mammalian orthologs (21). Hence, zfP2X4 structures are reasonable surrogates for modeling of the human variants of this channel.

P2X4 channels are trimeric (1) structures. zfP2X4 is a homotrimer (19, 22), with each subunit consisting of a transmembrane domain (TMD) and an extracellular ectodomain (Fig. 1). Each TMD contains two TM helices (TM1 and TM2). The TM2 of each sub unit together forms the TM pore that controls the gating of the channel (19, 22). ATP binds in an orthosteric binding site (Fig. 1) between the two neighboring subunits and facilitates a conformational transition i.e., from closed to open state, which was confirmed by the zfP2X4 crystal structures (19, 22). However, many details are still elusive including the number of ATP required to activate the channel and the role of ions in modulating the channel.

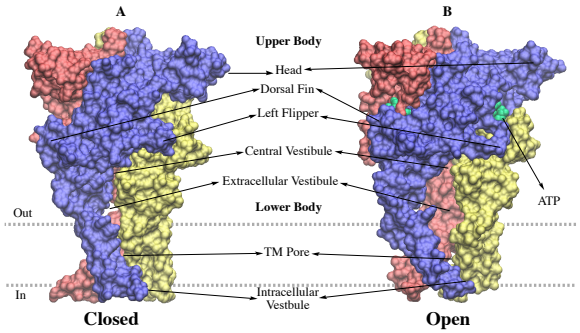

Figure 1: Closed (A) and open state (B) crystal structures of zfP2X4. The three isomers are colored blue, red and yellow, respectively. The closed structure is in apo form and ATP is binding in the open state structure between the isomers. ATP is shown in green. The TM pore, which is formed by the TM domain of each isomer, is the narrowest part of the channel. The TM pore is closed when deactivated and open when activated.

Ions play a critical role in normal functioning of many proteins (23–26). Divalent cations including zinc, magnesium, copper, cadmium, silver and mercury are reported to modulate the P2X receptors. For instance, it was demonstrated that zinc and copper modulate rat P2X4 receptors differently, i.e., zinc potentiates whereas copper inhibits ATP current (27, 28). Further, it was demonstrated via site directed mutagenesis the role of residue C132 in zinc potentiation (29), and residues D138 and H140 in copper inhibition in rat P2X4 receptors (29, 30). Similarly, it was reported that cadmium facilitates where as mercury inhibits ATP mediated currents in rat P2X4 receptors (31). Also, it was hypothesized that there are atleast three metal binding sites in P2X channels (31). Kasuya *et al.* reported an X-ray structure of Gulf Coast P2X receptor complexed with ATP and zinc ion (32). They have also reported two different metal binding sites, each for zinc and magnesium, respectively. Le *et al.* identified magnesium binding site near the ATP binding domain in the human P2X3 and demonstrated that magnesium enables ATP mediated activation of the channel. They have also proposed two different binding modes for magnesium in the presence and absence of ATP (33). The impact of divalent ions is not uniform among all P2X receptors. For example, it was proposed that magnesium does not have a role in P2X2 and P2X4, where as in P2X1 and P2X3 it does coordinate ATP binding (34). As explained above monovalent ions including sodium and potassium are permeable through all seven P2X receptors. Studies have reported that monovalent ions potassium and sodium modulate the human P2X7 receptor-operated single channel currents (35). This study also reported a binding site for sodium on the extracellular side. One study demonstrated a modulatory role of protons in rat P2X7 (36).

MD simulations enable studying the structural and functional aspects of membrane proteins at an atomic level (24). The

P2X4 computational studies conducted thus far are either based on short nanosecond level unbiased MD simulations or enhanced MD simulations and were only successful in implicating either a part of a channel or a particular residue or interaction in activation (37–44), thus its gating dynamics remain unresolved. A complete rigorous atomic level description of the channel activation is warranted. Hence, using microsecond level equilibrium MD simulations we studied (a) the number of ATP required to activate the channel and (b) the binding sites of monovalent/divalent ions and their potential role in modulating the zfP2X4 channel. Based on ≈13.5 μs of MD simulation data we show that minimum two ATP are required to activate zfP2X4. Additionally, we identified two metal binding sites in zfP2X4, similar to gulf coast P2X.

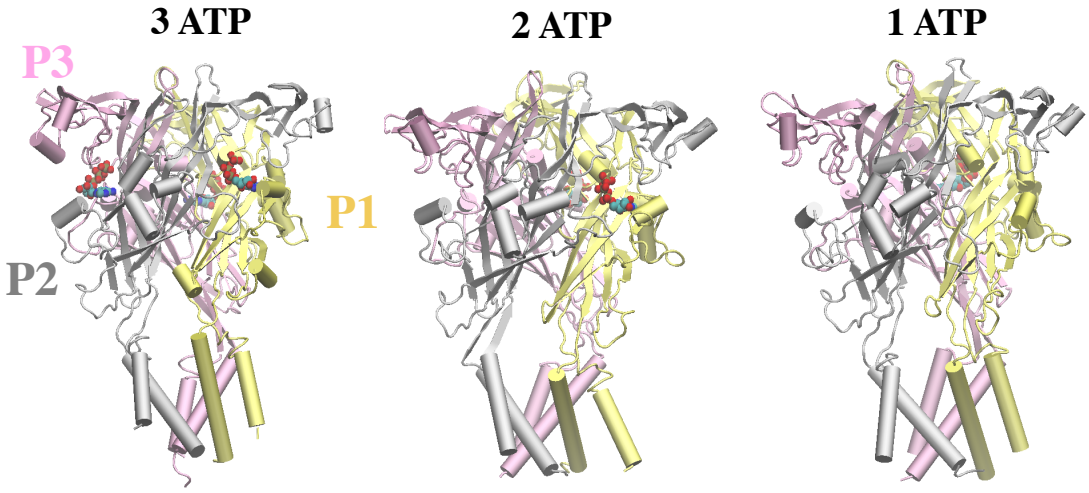

Figure 2: The three zfP2X4 structures studied. P1, P2 and P3 domains are colored yellow, grey and magenta, respectively. ATP molecules are shown as ball-and-stick representation. 1-ATP: ATP binds between P1 and P3 domains; 2-ATP: ATP binds between P1, P2 and P1, P3 domains. Side views of all three structures are shown.

2 METHODS

2.1 Molecular dynamics simulations

The open state crystal structure of zfP2X4 bound with three ATP molecules (PDB: 4DW1 (20)) was utilized for this study. Initially, the open state zfP2X4 crystal structure was downloaded from the crystal data bank and all waters were removed. The two and one ATP bound open state zfP2X4 systems were generated by deleting ATP from the three ATP bound crystal structure. All three systems were further processed and built for the MD simulation using the CHARMM-GUI web server (45, 46). Each system was placed in the POPC bilayer and solvated using the TIP3P water (47), and K^+ and chloride (Cl^-) ions were added to balance the charges as well as to attain a concentration of 0.15 M. Each system contains one P2X4 protein, ≈42,425 TIP3P water molecules, ≈388 POPC lipid molecules, 0.15 M KCl and 3/2/1 ATP molecules. The size of each system is $\approx 155 \times 160 \times 170$ Å^3 and the total number of atoms in each system is ≈195,116. Amber force-field (ff12SB) (48) was used to treat the entire system. Each system was energy minimized for 100,000 steps using conjugate gradient algorithm (49), and further relaxed in a multistep procedure (which spans for ≈1.5 ns), wherein the lipid tails, protein side chains, and backbone were restrained and then released in a step wise manner as explained elsewhere (45) in the NVT ensemble. Further, production simulations were conducted under

periodic boundary conditions in NPT ensemble. Three replicas of each system were carried, each replica for ~ 1 μs ($1\mu s \times 3$ trials $\times$ 3 systems = $9\mu s$). AMBER16 (50) was used for conducting the MD simulations. A 2 fs time step was used for the initial relaxation as well for the follow up production simulations. Temperature was maintained at 310 K using langevin thermostat and Nose-Hoover Langevin piston method was used to maintain a 1 atm pressure (51, 52). The non-bonded interactions were cut-off at 12 Å and the particle mesh Ewald (PME) method (53) was used to treat the long range electrostatics. Trajectories were saved every 20 ps. The SHAKE algorithm was used to constrain the hydrogen bonds (54).

In addition, all three systems described above are re-simulated (three replicas for each system) again but with the Mg^{2+} ions docked near the site of ATP binding as described in the references (32, 33). Please note that in the 2-ATP and 1-ATP systems Mg^{2+} was only docked to the sites that contains ATP. An additional 2-ATP and 1-ATP system were generated but with Mg^{2+} docked in all three domains irrespective of presence of ATP molecules. Overall, five Mg^{2+} docked open state zfP2X4 systems were modeled for MD simulations; a 3-ATP system with Mg^{2+} found at each docking site, two 2-ATP systems, and two 1-ATP systems. The 2-ATP and 1-ATP had one system each with Mg^{2+} docked in all three domains and one system each where Mg^{2+} only docked in domains where ATP is present. All simulations were conducted on a local GPU cluster.

Data analysis was conducted using VMD and its various plugins (55) and five data points per each ns was used for analysis. Simulation input files and generated data are available upon request.

3 RESULTS AND DISCUSSION

To study the ATP activation of P2X4, three open state P2X4 systems, each docked with three (3-ATP), two (2-ATP) and one ATP (1-ATP) molecules were simulated via unbiased MD simulations. An open state zfP2X4 crystal structure bound with three ATP (56) was utilized as a starting structure for this study. All three systems reached an apparent steady state at around 4 Å after 700 ns as evidenced by the backbone RMSDs (Fig. S1J). The backbone RMSD of the TMDs that form the TM pore were stabilized after 700 ns (Fig. S1 D-I) as well in all three systems (≈5-6 Å).

3.1 Two ATP molecules are atleast required to activate the zfP2X4

P2X receptors are activated by ATP facilitating the channel opening and transporting of the cations including K^+, sodium (Na^+) and Ca^{2+} across the biological membrane. ATP binds in the ectodomain and facilitate opening of the narrowest part of the channel (TM pore) formed by the TMD. P2X receptors are trimeric (homo/hetero) and are capable of binding three ATP molecules in the ectodomain (56). However, the minimum number of ATP required to activate the P2X receptors is still debated, particularly the P2X4s. Therefore, to study this aspect in detail we simulated three zfP2X4 open state receptors each docked with one, two and three ATP molecules, respectively. Since the activation of the channel opens the TM pore, we measured the pore radius as a function of the simulation time Fig. S2. Pore radius was estimated as the distance of C_α of L316 to the center of the TM pore. L316 was reported as the narrowest part of the TM pore (Fig. 3) (56). The TM pore of the 1-ATP system collapsed immediately (within the first 5 ns), where as the 2- & 3-ATP systems resisted the pore collapse hinting that at-least 2-ATP are required to activate the zfP2X4 channel. The average pore radius in the case of 1-ATP system was ≈3.8 Å (Fig. 3), where as in the case 2- and 3-ATP systems it was always ≥5.8 Å (Fig. 3), except for one 3-ATP trail (Fig. S2). Note that the

open zfP2X4 channel was used a starting system for all these simulations.

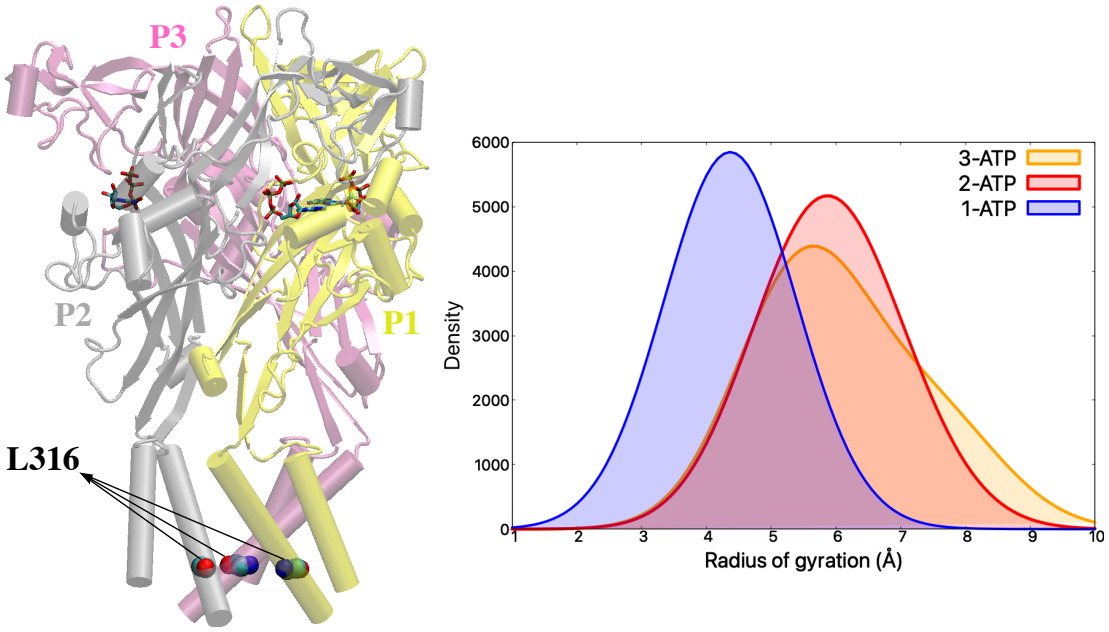

Figure 3: Density plot of radius of gyration (R_g). 1-ATP, 2-ATP and 3-ATP systems are colored blue, red and orange, respectively. L316 of the three isomers were used for the calculation of radius of gyration (R_g)(shown in left panel). Only C_α atoms of L316 were considered. The outliers were not considered for plotting the densities for clarity purpose .

3.2 Two metal binding sites were identified in zfP2X4

Ions are key for normal functioning of various proteins/receptors in humans. Particularly in P2X receptors, a range of cations bind and modulate their structure, dynamics and function. Studies have reported that divalent cations such as magnesium, zinc, copper and cadmium modulate P2X receptors (27, 28, 31–34). Studies have also identified the role of external monovalent cations in modulating P2X7 receptors, particularly potassium and sodium (35). A sodium binding site has also been identified in P2X7 in the same study. Given their importance, the role of cations have been investigated in this study in zfP2X4. We have identified two metal binding sites in the zfP2X4, similar to what was observed in the gulf coast P2X (32). The first metal binding site (MBS1) was identified at the intersection of three isomers in the upper part of the ectodomain (Fig. 4C). K^+ ions were found binding in the MBS1 and coordinating the three isomers via interacting with the polar (such as S101 and Y99) and negatively charged (such as E98, D99 and D323) residues of the protein (Fig. 4C,D). Further, the number of K^+ binding in the MBS1 (i.e., the number of K^+ ions that are within 8 Å of all three isomers in the vestibule) as a function of simulation time were estimated. On average two to three K^+ ions were consistently present in MBS1 in the 3-ATP and 2-ATP systems, whereas in the 1-ATP system they reduced from three to one with time (Fig. 5A). We hypothesize that this is due to the collapse of the channel in the 1-ATP system, thus collapsing MBS1. This supports our claim that atleast two ATP are required to activate the channel (or to keep the TM pore open). Earlier studies reported that zinc (Zn^{2+}) binding in the MBS1 potentiates ATP mediated currents in the gulf coast P2X channel through allostery (32). In the MBS1 residues that interact with the potassium ions are

E98, D99, Y99, S101 and D323. This is a highly conserved site across the P2X4 receptors and residues that are interacting with the zfP2X4 are similar to other P2X receptors (32).

The second metal binding site (MBS2) was identified near the ATP binding sites, which were present at the intersection of two neighboring isomers in the ectodomain (Fig. 4A). Several reports suggested that MBS2 was occupied by the Mg^{2+} ions (32, 33), coordinating the binding of ATP to the P2X2 and p2X4 receptors. In this study we have identified that K^+ ions were occupying the MBS2 and interacting with the ATP (Fig. 4A). Further, we estimated that atleast one K^+ ion was binding in the MBS2 (Fig. 5B-D). Additionally, we identified correlation between ATP binding to the channel and K^+ ions binding to the MBS2, i.e., when no ATP binds in a ATP binding site no K^+ ions binds to the respective MBS2, and vice versa. For instance, in the 3-ATP system, three ATP molecules binds to the three ATP binding sites and subsequently we observed K^+ ions binding to all three MBS2s. However, in the case of 2-ATP system K^+ ions were binding near the two ATP binding sites that were occupied by ATP but not near the ATP binding site that was not occupied with ATP (i.e., site between domains P2 and P3) (Fig. 5 B-D). Similarly in the 1-ATP system, K^+ was binding in the MBS2 adjacent to the site occupied with ATP (i.e., between the domains P1 and P3) and absent in the other two MBS2 sites. This is in contrast to the hP2X3, in which Mg^{2+} ions binds to all three MBS2s irrespective of ATP binding to the ATP binding sites (33). In the MBS2, residues primarily interacting with the K^+ ions were D145 and E171 (Fig. 4B). This is similar to others including gulf coast P2X (32) and hP2X3 (33).

It has been reported that ions binding to the MBS2 in different P2X receptors have diversified roles. For instance, magnesium binding to the MBS2 modulates the ATP mediated gating of P2X2 and P2X4 but not in P2X1 and P2X3 (32). Similarly, it was demonstrated that zinc binding to this site do not show potentiation of ATP mediated currents in gulf coast P2X (32). Further studies are required to establish the functional role of various ions binding to these two metal binding sites in zfP2X4, including the significance of various residues.

4 CONCLUSION

zfP2X4 is a homologue of human P2X4 and thus could provide critical insights into the P2X4-dependent progression of neuropathic pain. In this report we studied via MD simulations the activation of zfP2X4 by ATP and show that atleast two ATP molecules are required to activate the zfP2X4. We also identified two metal binding sites in the zfP2X4 similar to other P2X receptors such as gulf coast P2X. The first metal binding site is located at the intersection of three isomers in the upper part of the vestibule and the second metal binding site is located near the ATP binding site. We have identified K^+ ions binding to both the metal binding sites. The first metal binding site is dominantly occupied with negatively charged and polar residues thereby facilitating the binding of metal cations. K^+ ions binding in the second binding site is coordinating the binding of ATP with the receptor. Further studies are required to understand the role of ions binding to these two binding sites given the divergent role of different ions at different P2X receptors. The information gained from this study will help design strategies aimed at manipulating P2X receptors via small molecule modulators to treat diseases such as multiple sclerosis, neuropathic pain, thrombus, and rheumatoid arthritis (18).

5 AUTHOR CONTRIBUTIONS

KI conducted simulations, analyzed the data and wrote the manuscript. PKH designed the project and wrote the manuscript.

6 ACKNOWLEDGMENTS

Research reported in this publication was supported by the Maximizing Investigators' Research Award (MIRA) (R35) from the National Institute of General Medical Sciences (NIGMS) of the National Institutes of Health (NIH) under grant number R35GM124977. This work used the Extreme Science and Engineering Discovery Environment (XSEDE) (57), which is supported by National Science Foundation grant number ACI-1548562.

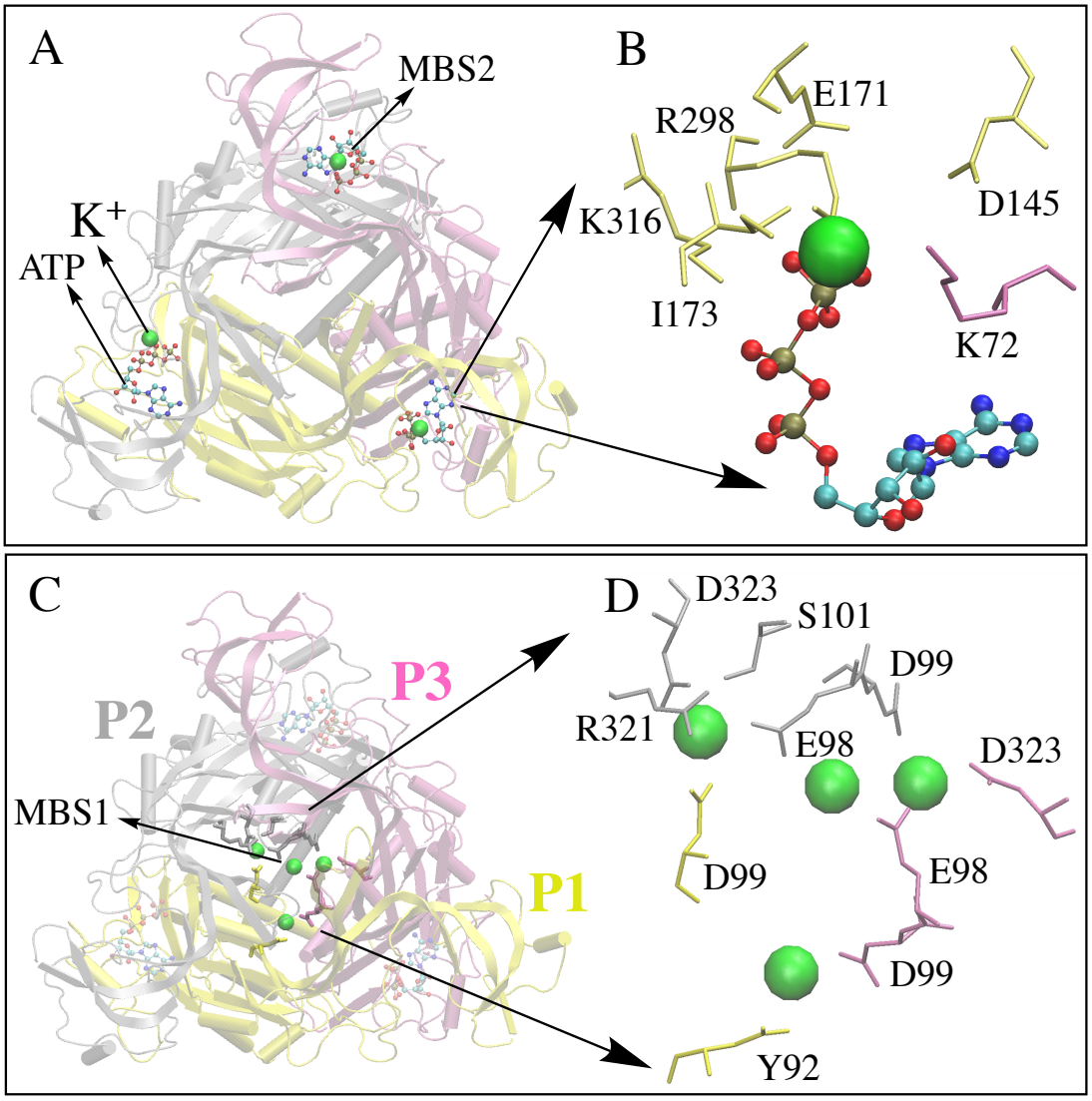

Figure 4: Metal binding sites 1 & 2 in the zfP2X4 (3-ATP system). **A** K^+ within 5 Å of ATP and 5 Å of protein in the metal binding site 2 (MBS2) are shown. P1, P2 and P3 are the individual isomers and are colored yellow, grey and magenta, respectively. **B** MBS2 between P1 and P3 shown in close-up. Green spheres are K^+ ions. ATP are shown as ball stick models. Residues within 5 Å of ions are shown. Residues are colored according to the respective domains they belong. **C** K^+ ions binding in the metal binding site 1 (MBS1) coordinating the three isomers inside the vestibule. Ions within 8 Å of all three isomers inside the vestibule are considered. **D** MBS1 close-up view. Top view of protein is shown in both A and C.

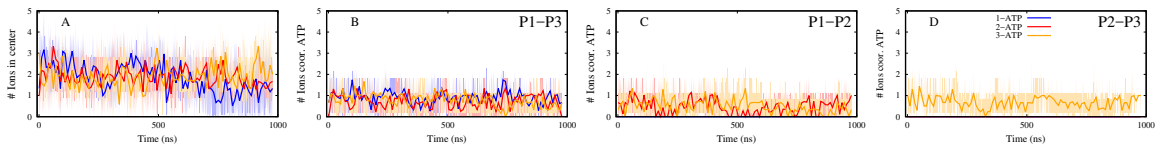

Figure 5: **A** Average number of K^+ ions binding in the MBS1 located at the intersection of three isomers in the vestibule. Ions within 8 Å of all three isomers inside the vestibule are shown. **B-D** Average number of K^+ ions binding in the MBS2s located between the isomers P1,P3 (B), P1,P2 (C) and P2,P3 (D). Ions within 5 Å of both the ATP and protein are estimated. 1-, 2-, and 3-ATP systems are colored blue, red and orange, respectively. Average and standard of the three MD trials are shown.

BIBLIOGRAPHY

1. Kaczmarek-Hájek, K., É. Lörinczi, R. Hausmann, and A. Nicke, 2012. Molecular and functional properties of P2X receptors—recent progress and persisting challenges. *Purinergic signalling* 8:375–417. 1

2. Bo, X., M. Kim, S. L. Nori, R. Schoepfer, G. Burnstock, and R. A. North, 2003. Tissue distribution of P2X 4 receptors studied with an ectodomain antibody. *Cell and tissue research* 313:159–165. 1

3. Rothwell, S. W., P. J. Stansfeld, L. Bragg, A. Verkhratsky, and R. A. North, 2014. Direct Gating of ATP-activated Ion Channels (P2X2 Receptors) by Lipophilic Attachment at the Outer End of the Second Transmembrane Domain. *Journal of Biological Chemistry* . 1

4. Khadra, A., Z. Yan, C. Coddou, M. Tomic, A. Sherman, and S. S. Stojilkovic, 2012. Gating properties of the P2X2a and P2X2b receptor channels: Experiments and mathematical modeling. *The Journal of general physiology* 139:333–348.

5. Shen, J.-B., 2006. Extracellular ATP-stimulated current in wild-type and P2X4 receptor transgenic mouse ventricular myocytes: implications for a cardiac physiologic role of P2X4 receptors. *The FASEB Journal* 20:277–284. 1

6. North, R. A., 2002. Molecular Physiology of P2X Receptors. *Physiological Reviews* 82:1013–1067. 1

7. Shigetomi, E., and F. Kato, 2004. Action potential-independent release of glutamate by Ca2+ entry through presynaptic P2X receptors elicits postsynaptic firing in the brainstem autonomic network. *Journal of Neuroscience* 24:3125–3135.

8. Koshimizu, T.-a., F. Van Goor, M. Tomić, A. O.-L. Wong, A. Tanoue, G. Tsujimoto, and S. S. Stojilkovic, 2000. Characterization of calcium signaling by purinergic receptor-channels expressed in excitable cells. *Molecular pharmacology* 58:936–945. 1

9. Solini, A., E. Santini, D. Chimenti, P. Chiozzi, F. Pratesi, S. Cuccato, S. Falzoni, R. Lupi, E. Ferrannini, G. Pugliese, et al., 2007. Multiple P2X receptors are involved in the modulation of apoptosis in human mesangial cells: evidence for a role of P2X4. *American Journal of Physiology-Renal Physiology* 292:F1537–F1547. 1

10. Baxter, A. W., S. J. Choi, J. A. Sim, and R. A. North, 2011. Role of P2X4 receptors in synaptic strengthening in mouse CA1 hippocampal neurons. *European Journal of Neuroscience* 34:213–220.

11. Kawano, A., M. Tsukimoto, T. Noguchi, N. Hotta, H. Harada, T. Takenouchi, H. Kitani, and S. Kojima, 2012. Involvement of P2X4 receptor in P2X7 receptor-dependent cell death of mouse macrophages. *Biochemical and biophysical research communications* 419:374–380.

12. Sadovnick, A. D., B. J. Gu, A. L. Traboulsee, C. Q. Bernales, M. Encarnacion, I. M. Yee, M. G. Criscuoli, X. Huang, A. Ou, C. J. Milligan, et al., 2017. Purinergic receptors P2RX4 and P2RX7 in familial multiple sclerosis. *Human mutation* 38:736–744. 1

13. Ulmann, L., H. Hirbec, and F. Rassendren, 2010. P2X4 receptors mediate PGE2 release by tissue-resident macrophages and initiate inflammatory pain. *The EMBO journal* 29:2290–2300. 1

14. Tsuda, M., K. Kuboyama, T. Inoue, K. Nagata, H. Tozaki-Saitoh, and K. Inoue, 2009. Behavioral phenotypes of mice lacking purinergic P2X 4 receptors in acute and chronic pain assays. *Molecular pain* 5:28. 1

15. Ulmann, L., J. P. Hatcher, J. P. Hughes, S. Chaumont, P. J. Green, F. Conquet, G. N. Buell, A. J. Reeve, I. P. Chessell, and F. Rassendren, 2008. Up-regulation of P2X4 receptors in spinal microglia after peripheral nerve injury mediates BDNF release and neuropathic pain. *Journal of Neuroscience* 28:11263–11268. 1

16. Tsuda, M., Y. Shigemoto-Mogami, S. Koizumi, A. Mizokoshi, S. Kohsaka, M. W. Salter, and K. Inoue, 2003. P2X 4 receptors induced in spinal microglia gate tactile allodynia after nerve injury. *Nature* 424:778. 1

17. Grimes, L., and M. T. Young, 2015. Purinergic P2X receptors: structural and functional features depicted by X-ray and molecular modelling studies. *Current medicinal chemistry* 22:783–98. 1

18. Wang, J., and Y. Yu, 2016. Insights into the channel gating of P2X receptors from structures, dynamics and small molecules. *Acta Pharmacologica Sinica* 37:44–55. 1, 4

19. Kawate, T., J. C. Michel, W. T. Birdsong, and E. Gouaux, 2009. Crystal structure of the ATP-gated P2X 4 ion channel in the closed state. *Nature* 460:592. 1

20. Hattori, M., and E. Gouaux, 2012. Molecular mechanism of ATP binding and ion channel activation in P2X receptors. *Nature* . 1, 2.1

21. Diaz-Hernandez, M., J. A. Cox, K. Migita, W. Haines, T. M. Egan, and M. M. Voigt, 2002. Cloning and characterization of two novel zebrafish P2X receptor subunits. *Biochemical and biophysical research communications* 295:849–853. 1

22. Hato, Z., D. Boda, and T. Kristof, 2012. Simulation of steady-state diffusion: Driving force ensured by dual control volumes or local equilibrium Monte Carlo. *The Journal of chemical physics* 137:54109. 1

23. van de Locht, M., S. Donkervoort, J. M. de Winter, S. Conijn, L. Begthel, B. Kusters, P. Mohassel, Y. Hu, L. Medne, C. Quinn, S. A. Moore, R. Foley, G. Seo, D. T. Hwee, F. I. Malik, T. Irving, W. Ma, H. Granzier, E.-J. Kamsteeg, K. Immadisetty, P. Kekenes-Huskey, J. R. Pinto, N. Voermans, C. G. Bönnemann, and C. A. Ottenheijm, 2021. Pathogenic variants in TNNC2 cause congenital myopathy due to an impaired force response to calcium. *The Journal of Clinical Investigation* . 1

24. Immadisetty, K., and J. D Madura, 2013. A review of monoamine transporter-ligand interactions. *Current Computer aided drug design* 9:556–568. 1

25. Immadisetty, K., and M. Moradi, 2020. Mechanistic picture for chemo-mechanical couplings in a bacterial proton-coupled oligopeptide transporter from Streptococcus thermophilus. *bioRxiv* .

26. Immadisetty, K., B. Sun, and P. Kekenes-Huskey, 2020. Structural determinants of calcium binding beyond the EF-hand binding site: a study of alpha parvalbumins. *bioRxiv* . 1

27. Acuña-Castillo, C., B. Morales, and J. P. Huidobro-Toro, 2000. Zinc and copper modulate differentially the P2X4 receptor. *Journal of neurochemistry* 74:1529–1537. 1, 3.2

28. Coddou, C., B. Morales, and J. P. Huidobro-Toro, 2003. Neuromodulator role of zinc and copper during prolonged ATP applications to P2X4 purinoceptors. *European journal of pharmacology* 472:49–56. 1, 3.2

29. Coddou, C., C. Acuña-Castillo, P. Bull, and J. P. Huidobro-Toro, 2007. Dissecting the facilitator and inhibitor allosteric metal sites of the P2X4 receptor channel: critical roles of CYS132 for zinc potentiation and ASP138 for copper inhibition. *Journal of Biological Chemistry* 282:36879–36886. 1

30. Coddou, C., B. Morales, J. González, M. Grauso, F. Gordillo, P. Bull, F. Rassendren, and J. P. Huidobro-Toro, 2003. Histidine 140 plays a key role in the inhibitory modulation of the P2X4 nucleotide receptor by copper but not zinc. *Journal of Biological Chemistry* 278:36777–36785. 1

31. Coddou, C., R. A. Lorca, C. Acuña-Castillo, M. Grauso, F. Rassendren, and J. P. Huidobro-Toro, 2005. Heavy metals modulate the activity of the purinergic P2X4 receptor. *Toxicology and applied pharmacology* 202:121–131. 1, 3.2

32. Kasuya, G., Y. Fujiwara, M. Takemoto, N. Dohmae, Y. Nakada-Nakura, R. Ishitani, M. Hattori, and O. Nureki, 2016. Structural Insights into Divalent Cation Modulations of ATP-Gated P2X Receptor Channels. *Cell Reports* 14:932–944. 1, 2.1, 3.2

33. Li, M., Y. Wang, R. Banerjee, F. Marinelli, S. Silberberg, J. D. Faraldo-Gómez, M. Hattori, and K. J. Swartz, 2019. Molecular mechanisms of human P2X3 receptor channel activation and modulation by divalent cation bound ATP. *eLife* 8:e47060. 1, 2.1, 3.2

34. Chataigneau, T., D. Lemoine, and T. Grutter, 2013. Exploring the ATP-binding site of P2X receptors. *Frontiers in cellular neuroscience* 7:273. 1, 3.2

35. Riedel, T., G. Schmalzing, and F. Markwardt, 2007. Influence of extracellular monovalent cations on pore and gating properties of P2X7 receptor-operated single-channel currents. *Biophysical journal* 93:846–858. 1, 3.2

36. Acuña-Castillo, C., C. Coddou, P. Bull, J. Brito, and J. P. Huidobro-Toro, 2007. Differential role of extracellular histidines in copper, zinc, magnesium and proton modulation of the P2X7 purinergic receptor. *Journal of neurochemistry* 101:17–26. 1

37. Du, J., H. Dong, and H.-X. Zhou, 2012. Gating mechanism of a P2X4 receptor developed from normal mode analysis and molecular dynamics simulations. *Proceedings of the National Academy of Sciences* 109:4140–4145. 1

38. Heymann, G., J. Dai, M. Li, S. D. Silberberg, H.-X. Zhou, and K. J. Swartz, 2013. Inter-and intrasubunit interactions between transmembrane helices in the open state of P2X receptor channels. *Proceedings of the National Academy of Sciences* 110:E4045–E4054.

39. Zhao, W.-S., J. Wang, X.-J. Ma, Y. Yang, Y. Liu, L.-D. Huang, Y.-Z. Fan, X.-Y. Cheng, H.-Z. Chen, R. Wang, et al., 2014. Relative motions between left flipper and dorsal fin domains favour P2X4 receptor activation. *Nature communications* 5:4189.

40. Turchenkov, D. A., and V. S. Bystrov, 2014. Conductance simulation of the purinergic P2X2, P2X4, and P2X7 ionic channels using a combined brownian dynamics and molecular dynamics approach. *The Journal of Physical Chemistry B* 118:9119–9127.

41. Huang, L.-D., Y.-Z. Fan, Y. Tian, Y. Yang, Y. Liu, J. Wang, W.-S. Zhao, W.-C. Zhou, X.-Y. Cheng, P. Cao, et al., 2014. Inherent dynamics of head domain correlates with ATP-recognition of P2X4 receptors: insights gained from molecular simulations. *PloS one* 9:e97528.

42. Pierdominici-Sottile, G., L. Moffatt, and J. Palma, 2016. The dynamic behavior of the P2X4 ion channel in the closed conformation. *Biophysical journal* 111:2642–2650.

43. Zhao, W. S., M. Y. Sun, L. F. Sun, Y. Liu, Y. Yang, L. D. Huang, Y. Z. Fan, X. Y. Cheng, P. Cao, Y. M. Hu, L. Li, Y. Tian, R. Wang, and Y. Yu, 2016. A highly conserved salt bridge stabilizes the kinked conformation of β2,3-sheet essential for channel function of P2X4 receptors. *Journal of Biological Chemistry* 291:7990–8003.

44. Wang, J., L. F. Sun, W. W. Cui, W. S. Zhao, X. F. Ma, B. Li, Y. Liu, Y. Yang, Y. M. Hu, L. D. Huang, X. Y. Cheng, L. Li, X. Y. Lu, Y. Tian, and Y. Yu, 2017. Intersubunit physical couplings fostered by the left flipper domain facilitate channel opening of P2X4 receptors. *Journal of Biological Chemistry* 292:7619–7635. 1

45. Jo, S., T. Kim, and W. Im, 2007. Automated builder and database of protein/membrane complexes for molecular dynamics simulations. *PLoS One* 2:e880. 2.1

46. Lee, L. C., G. S. Kassab, and J. M. Guccione, 2016. Mathematical modeling of cardiac growth and remodeling. *Wiley Interdisciplinary Reviews: Systems Biology and Medicine* 8:211–226. 2.1

47. Jorgensen, W. L., J. Chandrasekhar, J. D. Madura, R. W. Impey, and M. L. Klein, 1983. Comparison of Simple Potential Functions for Simulating Liquid Water. *Journal of Chemical Physics* 79:926–935. 2.1

48. Case, D., T. Darden, T. E. Cheatham, C. Simmerling, J. Wang, R. E. Duke, R. Luo, R. C. Walker, W. Zhang, and K. M. Merz, 2012. Amber 12. *University of California: San Francisco, CA* . 2.1

49. Reid, J. K., 1971. On the Method of Conjugate Gradients for the Solution of Large Sparse Systems of Linear Equations. *In* J. K. Reid, editor, Large Sparse Sets of Linear Equations, Academic Press, London, 231–254. 2.1

50. Case, D., R. Betz, D. Cerutti, T. Cheatham, T. Darden, R. Duke, T. Giese, H. Gohlke, A. Götz, N. Homeyer, S. Izadi, P. Janowski, J. Kaus, A. Kovalenko, T.-S. Lee, S. LeGrand, P. Li, C. Lin, T. Luchko, and P. A. Kollman, 2016. Amber 16. *University of California: San Francisco, CA* . 2.1

51. Martyna, G. J., D. J. Tobias, and M. L. Klein, 1994. Constant pressure molecular dynamics algorithms. *Journal of Chemical Physics* 101:4177–4189. 2.1

52. Feller, S. E., Y. Zhang, R. W. Pastor, and B. R. Brooks, 1995. Constant pressure molecular dynamics simulation: The Langevin piston method. *Journal of Chemical Physics* 103:4613–4621. 2.1

53. Darden, T., D. York, and L. Pedersen, 1993. Particle mesh Ewald: An Nlog(N) method for Ewald sums in large systems. *The Journal of chemical physics* 98:10089–10092. 2.1

54. Ryckaert, J.-P., G. Ciccotti, and H. J. C. Berendsen, 1977. Numerical integration of the cartesian equations of motion of a system with constraints: molecular dynamics of n-alkanes. *Journal of Computational Physics* 23:327–341. 2.1

55. Humphrey, W., A. Dalke, and K. Schulten, 1996. VMD: visual molecular dynamics. *Journal of Molecular Graphics* 14:33–38. 2.1

56. Hattori, M., and E. Gouaux, 2012. Molecular mechanism of ATP binding and ion channel activation in P2X receptors. *Nature* 485:207. 3, 3.1

57. Towns, J., T. Cockerill, M. Dahan, I. Foster, K. Gaither, A. Grimshaw, V. Hazlewood, S. Lathrop, D. Lifka, G. D. Peterson, R. Roskies, J. R. Scott, and N. Wilkens-Diehr, 2014. XSEDE: Accelerating Scientific Discovery. *Computing in Science & Engineering* 16:62–74. 6

7 SUPPLEMENTARY MATERIAL

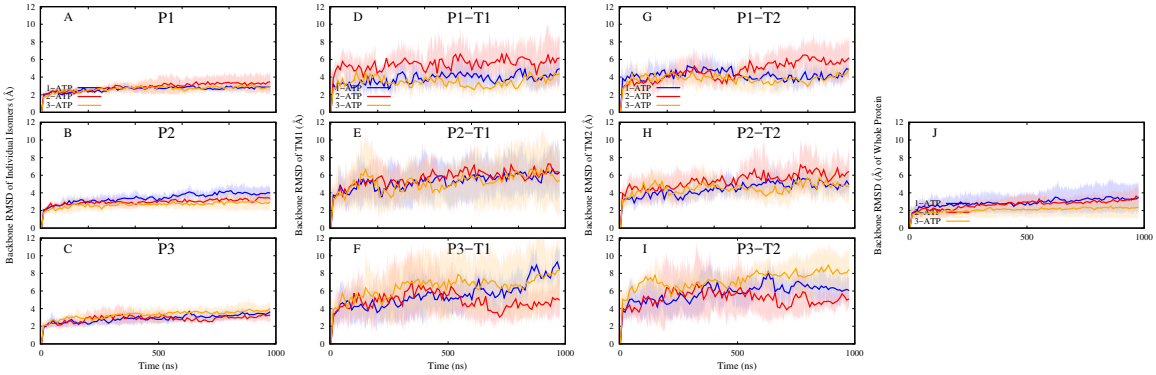

Figure S1: Backbone RMSD vs. Time. P1, P2 and P3 corresponds to the three isomers. TM1 and TM2 are transmembrane helices 1 and 2 of each isomer. **A-C** RMSDs of the three isomers. **D-F** RMSDs of TM1s of the three isomers. **G-I** RMSDs of TM2s of the three isomers. **J** RMSD of all three isomers of each zfP2X4 combined. Average of three MD trials of each system is shown and the error bars (i.e., standard deviation) are shaded.

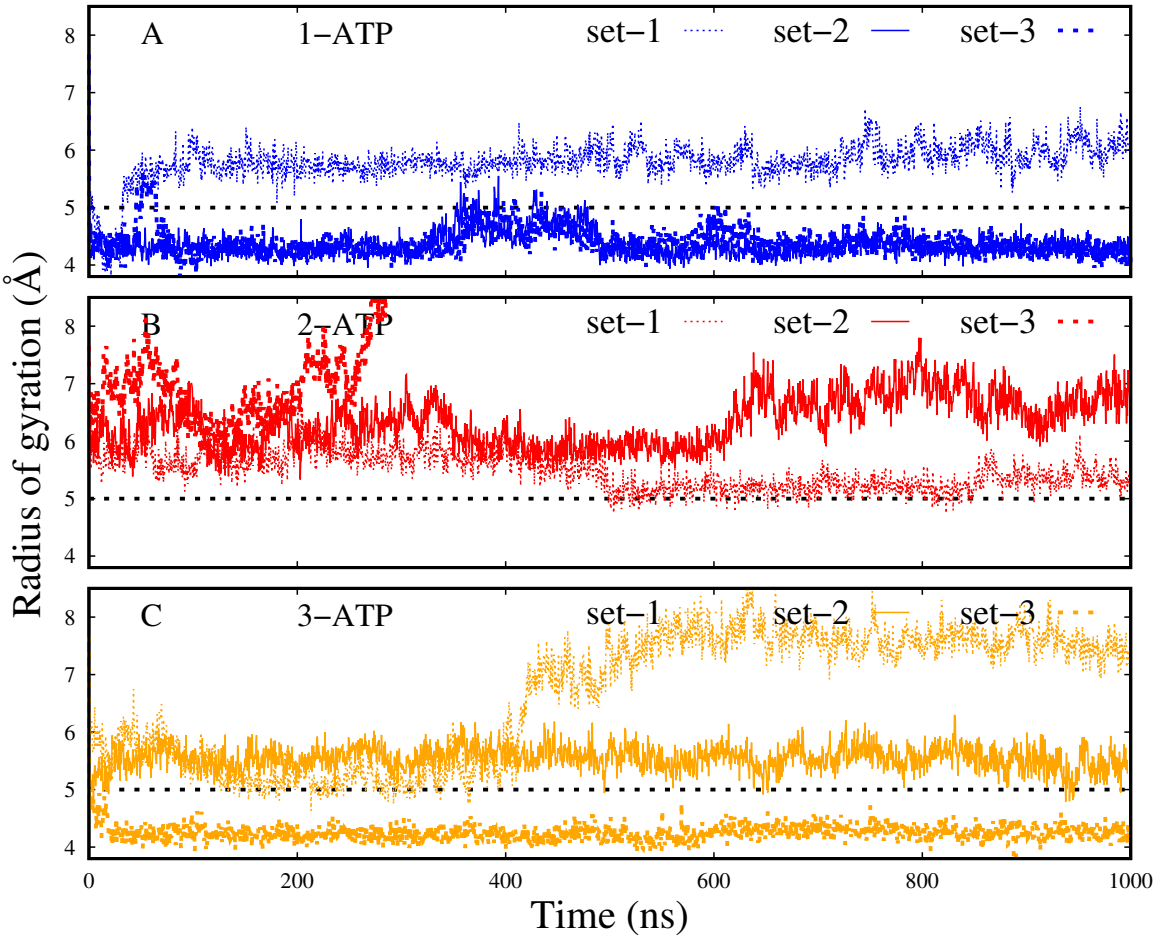

Figure S2: Radius of gyration vs. time. 1-, 2-, and 3-ATP systems are colored blue, red and orange, respectively. Dotted horizontal line at Y=5 separates 1-ATP system with the other two sytems. R_g of 1-ATP systems were less than 5 Å, except for one outlier (set-1). On the other hand the R_g of 2- & 3-ATP systems are greater than 5 Å, except for one outlier in the 3-ATP system (set-3).

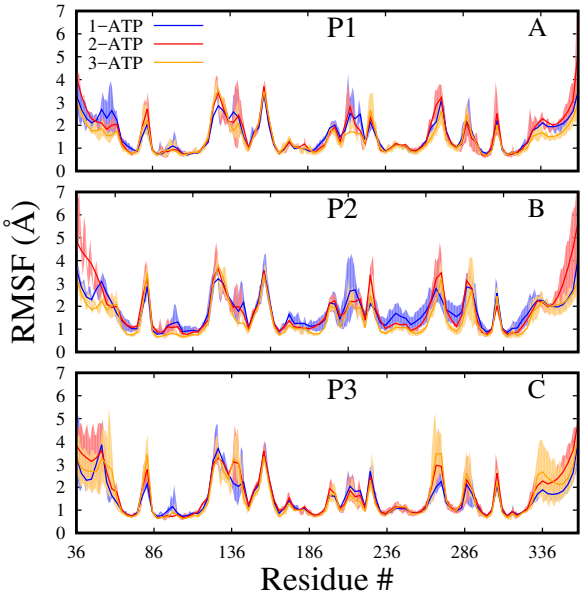

Figure S3: Root mean squared fluctuations (RMSF) vs. Residue Number. Only C_α atoms are considered. P1, P2 and P3 refers to the individual isomers. P2 isomer of 1-ATP system is more dynamic than the other two, particularly residues 230-286. 1-, 2-, and 3-ATP systems are colored blue, red and orange, respectively. Average and standard of the three MD trials are shown.

ACRONYMS

Ca^{2+} calcium. 1, 4

Cl^{-} chloride. 3

K^{+} potassium. 1, 3–6, 8

MD molecular dynamics. 1–4, 8, 14, 16

Mg^{2+} magnesium. 1, 4, 6

Na^{+} sodium. 4

R_g radius of gyration. 5, 15

RMSF Root mean squared fluctuations. 16

TMD transmembrane domain. 2, 4

zfP2X4 zebrafish P2X4. 1–6, 8, 14

Zn^{2+} zinc. 5